Volumetric Properties of Gaseous Acetone

L. N. ANDERSON[1], A. P. KUDCHADKER, and P. T. EUBANK
Department of Chemical Engineering, Texas A&M University, College Station, Tex. 77843

Experimental compressibilities of gaseous acetone for the temperature range 25° to 150° C. at 25° C. intervals were obtained from a Burnett *PVT* apparatus for the pressure range 1 to 105 p.s.i.a. Second, third, and fourth virial coefficients are presented which provide an adequate fit of the experimental data. Computed values of the equilibrium constant for dimerization are in good agreement with those calculated from heat capacity measurements. The experimental data are compared with the Stockmayer intermolecular potential energy model and the polar correlation of Eubank and Smith. The experimental apparatus, errors in the compressibility results, and acetone purity are discussed. Equations for correction of Burnett *PVT* data for adsorption of gas molecules to the metallic walls of the cell are presented.

THE compressibility factor

$$Z = \frac{P\bar{V}}{RT} = 1 + B'P + C'P^2 + D'P^4 + \ldots \quad (1)$$

is used as a measure of deviation from ideality. B', C', and D' are the second, third, and fourth Berlin virial coefficients. Volumetric or PVT data for inert gases such as helium are well described by a linear variation of Z with P

$$Z_0 = 1 + B'P \quad (2)$$

to moderate pressures (2000 p.s.i.a.) at usual temperatures (0° to 200° C.). The compressibility, Z_0, of inert gases may also be accurately described from the corresponding states theory

$$Z_0 = Z_0(P_r, T_r) \quad (3)$$

Pure hydrocarbon gases required terms beyond the second of Equation 1 to describe volumetric properties over the above pressure and temperature ranges. The gas molecules are nonpolar but acentric, unlike the inert gases. Compressibilities are well described by the equation of Pitzer,

$$Z = Z_0 + \omega Z_1 \quad (4)$$

where $\omega = -\log P_r - 1.000$ at $T_r = 0.7$ and $Z_1 = Z_1(P_r, T_r)$.

Polar gases show further deviation from ideality because of the attractive forces between polar molecules due to permanent dipoles. Such attraction causes a decrease in the compressibility. Association of the gas molecules occurs readily and is caused by chemical bonding or hydrogen bonding and/or physical attraction due to electrostatic effects. Association may appear in the form of hydrogen bonding or it may not, as with acetone. Compressibilities may be correlated by the equation of Eubank and Smith (*8*)

$$Z = Z_0 + \omega Z_1 + P^* Z_2 \quad (5)$$

where $P^* = c\mu^{*5.3}$, $\mu^* = \mu/(\epsilon\sigma^3)^{1/2}$, and $Z_2 = Z_2(P_r, T_r)$. The nonpolar contribution, $Z_0 + \omega Z_1$, is based on the nonpolar homomorph of the polar compound; for the organic alcohols, ketones, and ethers, the homomorphs are found by replacing the OH or O group by the CH_2 or CH_3 group. The constant c depends only on the compound class and is unity for alcohols, 0.7 for ketones, and 0.3 for ethers.

The lack of acetone compressibility data is typical of polar gases. No significant work is known to exist above 1-atm. pressure. Data below 1-atm. pressure aimed at the determination of the second virial coefficient have been reported by Eucken and Meyer (*9*), Lambert, Roberts, Rowlinson, and Wilkinson (*13*), Bottomley and Spurling (*5*, *6*), Abbott (*1*), Zaalishvili and Kolysko (*29*, *30*), and Zaalishvili and Belousova (*28*). Kobe and Pennington (*12*) determined vapor heat capacities and heats of vaporization. Literature vapor pressure data used in the present work together with a complete review of volumetric and thermodynamic results for acetone may be found in the report of Barb (*4*).

EXPERIMENTAL APPARATUS

A Burnett PVT apparatus as shown by Figures 1 and 2 was used. Because this apparatus is similar to those of Silberberg, McKetta, and Kobe (*22*), Mueller, Leland, and Kobayashi (*18*), and Suh and Storvick (*25*), an abbreviated description concerned chiefly with unusual features is given.

Burnett Cell. The cell was machined from 303 stainless steel with the volumes V_1 and V_2 approximately 700 and 300 cc., respectively. The expansion valve (valve No. 2, Figure 2) was the constant volume type. A differential pressure indicator (DPIB) separated the experimental gas in the constant temperature bath from dry nitrogen which transmitted the pressure outside the bath. While not necessary for the present work, operation at extreme temperatures often necessitates placing DPIB outside the bath; Burnett compressibility data are corrected for the resulting error according to the method derived in Appendix A (on deposit with the American Documentation Institute).

Pressure Measurement. Nitrogen transmitted the experimental gas pressure directly to a quartz Bourdon gage (precision pressure gage) when the pressure was below 24 p.s.i.a. The gage which was permanently evacuated for direct absolute pressure measurement was originally calibrated by the manufacturer and later by a competitor. In both cases, the primary pressure standard was an in-

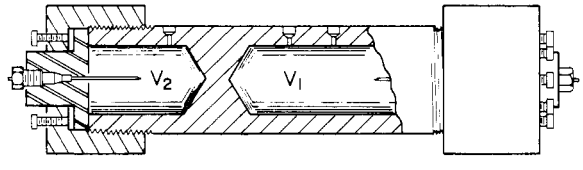

Figure 1. Burnett cell

[1] Present address: Technical Center, Celanese Chemical Co., Corpus Christi, Tex.

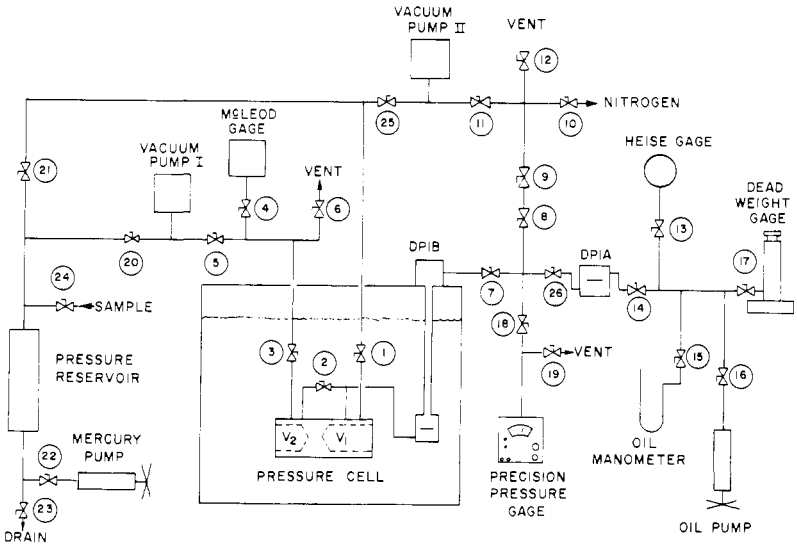

Figure 2. Schematic diagram of apparatus

clined, air-operated, dead-weight gage traceable to the National Bureau of Standards. For the pressure range of 1 to 24 p.s.i.a., gage readings were reproducible to ±0.0017 p.s.i. The maximum uncertainty in the calibration was ±0.0055 p.s.i.a. or 0.023% at the maximum pressure and ±0.0019 p.s.i. or 0.19% at the minimum pressure.

Pressures above 20 p.s.i.a. were measured with a dead-weight gage with a total maximum uncertainty of ±0.0061 p.s.i., including ±0.0040 p.s.i. from the atmospheric pressure measurement obtained from the quartz Bourdon gage. The dead-weight gage was calibrated by the manufacturer against a similar gage originally calibrated by NBS. A second differential pressure indicator (DPIA) was used to transmit pressure from the nitrogen to the dead-weight gage oil.

With reference to Figure 2, DPIA is a Ruska differential pressure indicator, Model 2411.1, sensitivity 0.0002 p.s.i. DPIB (Model 2416.1), also manufactured by Ruska, is of 0.0001 p.s.i. sensitivity. The gages are basically of the same design, but DPIB was especially equipped with a long vertical shaft to transmit the motion of the primary diaphragm, which is in contact with the experimental gas in the bath, to the secondary diaphragm located on top of the bath.

Temperature Measurement. A platinum resistance thermometer, used to measure the bath temperature near the cell, was calibrated by NBS at the triple point of water, the steam point, and the sulfur point. The uncertainty of the calibration at these points is less than ±0.0003°, ±0.0015°, and ±0.0003° C., respectively. Iron-constantan thermocouples entered the thermal wells of the Burnett cell to detect temperature differences between the bath and experimental gas. As indicated by a preliminary study, no temperature gradients in excess of 0.01° C. were found within the bath. This was due to the use of a Thermotrol temperature controller, three tubular heaters, and thorough bath mixing. The bath contained 30 gallons of Dow 710 silicone oil capable of sustained temperatures from 0° to 250° C. The over-all accuracy of the temperature measurement was considered to be 0.01° C.

Miscellaneous. A vacuum system capable of below 50 microns of Hg pressure was used, as shown by Figure 2. It was necessary to use liquid nitrogen in the cold traps associated with the vacuum pumps. The liquid charging system consisted of a gallon glass jar containing acetone, a pressure reservoir, a mercury pump, and a mercury probe. A precision cathetometer was used to determine the correct height of the dead weights relative to the piston height and the height of the reference levels of the differential pressure indicators.

The experimental apparatus has been described by Anderson (2, 3).

PURITY OF CHEMICALS

Helium for calibration of the apparatus was reported to be 99.99+% pure.

The original sample of acetone was donated by the Union Carbide Chemicals Co. from a special batch distillation run. The supplier reported the sample to be 99.81% pure by chromatographic analysis. The impurities were 0.11% isopropyl ether, 0.07% water, and 0.01% unidentified. No further purification was attempted. The acetone sample was received in a sealed 5-gallon can. Approximately 1 gallon of this sample was transferred under a nitrogen atmosphere to a dark brown reagent bottle (not shown). The bottle was connected to the sample valve (24) of Figure 2 and periodically supplied acetone to the previously evacuated pressure reservoir, a high pressure feed tank. With the above charging procedure, the acetone was exposed only to nitrogen at atmospheric pressure.

At the completion of the acetone investigation, the unused portion in the feed tank was analyzed by the Celanese Chemical Co. by gas chromatography. The result was 99.75% acetone, 0.15% isopropyl ether, 0.03% water, and 0.07% a collection of numerous compounds—many unidentified. The analysis of a sample taken from the Burnett cell at 175° C. is discussed in connection with the problem of association.

Purity of acetone and accuracy of pressure measurements were regarded as the major sources of error in the experimental compressibilities.

HELIUM CALIBRATION

A complete discussion of the standard Burnett calculational procedure has been provided by Silberberg, McKetta, and Kobe (22). For a given run at a set temperature a sequence of pressures, P_0, P_1, ... P_i, are obtained from which the apparatus constant

$$N = \frac{V_1 + V_2}{V_1} = \lim_{P_i \to 0} \frac{P_i}{P_{i+1}} \tag{6}$$

the initial pressure-compressibility ratio

$$\frac{P_0}{Z_0} = \lim_{P_i \to 0} P_i N^i \tag{7}$$

and the compressibility sequence, Z_0, Z_1, ... Z_i, may be

found. The latter result relies on the recursion relation

$$\frac{P_i}{P_{i-1}} = N \frac{Z_i}{Z_{i-1}} \qquad (8)$$

Three runs at both 50° and 150° C. were made with helium prior to the acetone investigation to test the apparatus against the results of other workers. The final apparatus constant was determined to be 1.43251 with negligible variation with temperature. Experimental compressibilities were fitted by Equation 2 to within the estimated maximum experimental uncertainty of 0.05%. The resultant Berlin second virial coefficients are compared with other investigations in Table I. Helium is seen to be a good calibration gas because of extensive literature values, linearity of Z *vs.* P, and low values of second virial coefficient which test apparatus sensitivity.

ACETONE DATA TREATMENT

Two unusual observations were detected during the acetone investigation, which covered a temperature range of 25° to 150° C. First, the time to reach equilibrium between expansions was 10 to 12 hours instead of the usual 1 to 2 hours for helium. Second, values of the apparatus constant, N, determined from the zero pressure limit of the pressure ratio, Equation 6, at 25° C. were significantly less than the above, constant value for helium. Values of N computed from this limit for acetone increased with temperature and were at 150° C. only slightly less than the helium value. Values of N from acetone data were thus considered unreliable and discarded in favor of the helium value in subsequent computations. Graphs of P_iN^i *vs.* P_i, of which Figure 3 is an example, were next prepared. At the highest pressure P_0 of 51.1 p.s.i.a. for this run at 100° C., the curve is steep, indicating association, the saturation pressure is 54.0 p.s.i.a. (*11*). Near a pressure of 17 p.s.i.a. the curve shows an unusual inflection point at lower pressure, and appears to approach zero pressure asymptotic to the P_iN^i axis, which prevents meaningful extrapolation in determination of (P_0/Z_0) according to Equation 7.

Two phenomena, association and adsorption, were originally considered as possible causes for the low-pressure behavior. Application of a simple dimerization model as used by Lambert *et al.* (*13*) to the sequential Burnett equations showed that the apparatus constant is unaffected. The limiting value of the P_iN^i product is increased, though not infinite and, no inflection in the P_iN^i *vs.* P_i curve is predicted. Thus, association—a dominating influence on the compressibility of acetone at the temperatures investigated—was discarded as the cause of the decrease of the apparatus constant and low-pressure behavior of the P_iN^i curve. The isothermal adsorption model of Langmuir (*14*) correctly predicted the shift in the apparatus constant and the behavior shown by Figure 3. Coupling of the Langumir model with the sequential Burnett equations is presented in Appendix B (on deposit with ADI), with the result that

Table I. Comparison of Second Virial Coefficient Data for Helium

$B^1 \times 10^4$ p.s.i.a. $^{-1}$

Ref.	50° C.	150° C.
Michels and Wouters (*15*)	0.297	0.217
Holborn and Otto (*10*)	0.301	...
Wiebe, Gaddy, and Heins (*27*)	0.293	...
Moreland (*17*)	...	0.222
This work	0.308	0.219

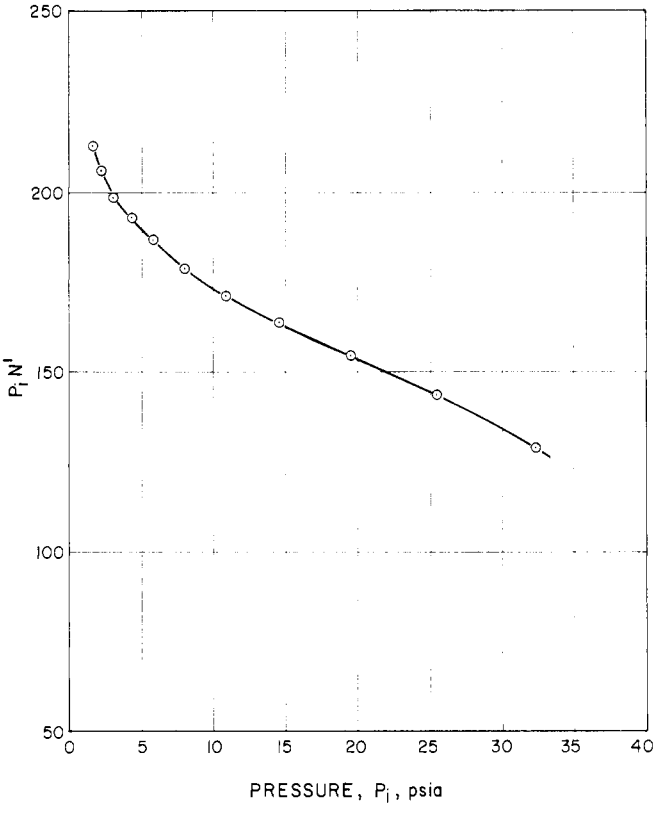

Figure 3. Uncorrected P_iN^i graph for acetone, 100° C., Run III

$$U_0 = \frac{N + S_a W}{1 + W} \qquad (9)$$

where U_0 is the limiting value of the pressure ratio at a given temperature, S_a is the ratio of the total surface area of $V_1 + V_2$ to the surface area of V_1, and W is an adsorption constant which is determined from Equation 9 as a function of temperature.

If V_1 and V_2 were simple capped cylinders, $S_a < N$, and $U_0 > N$, which is counter to the experimental observation that $N > U_0$. This paradox disappears when the surface area of tubing and cavities (such as DPIB) associated with V_1 and the tubing associated with V_2 are considered. The estimated values are $V_1 = 41.6$, $V_2 = 17.8$, area of cylinder $V_1 = 72.5$, area of cylinder $V_2 = 37.8$, tubing area associated with $V_1 = 18.8$, tubing area associated with $V_2 = 4.2$, area of DPIB cavity = 15.1, and V_1 associated cavity in expansion valve = 2.3 (all values in square or cubic inches). The area ratio S_a is then 1.388 rather than 1.521 and $S_a < N$ or $N > U_0$. Compressibilities are corrected according to the equations

$$\frac{1}{Z_i} = \frac{P_0/Z_0}{N^i P_i} + h_i \qquad (10)$$

and

$$h_i = W \sum_{j=1}^{i} N^j \left[\frac{P_{i-j}}{P_{i-j-1}(1 + bP_{i-j})} - \frac{S_a}{1 + bP_{i-j+1}} \right] \frac{P_{i-j+1}}{P_i} \qquad (11)$$

where b is a second adsorption constant determined by the ability of the correction h_i to provide the compressibility sequence with a zero pressure intercept of unity. The value of (P_0/Z_0) is found from

$$\frac{P_0}{Z_0} = \left(\frac{1}{Z_i} - h_i \right) P_i N^i \qquad (12)$$

or

$$\frac{P_0}{Z_0} = \lim_{P_i \to 0} [1 - h_i] P_i N^i \qquad (13)$$

The Langmuir model predicts all observed effects and their variation with temperature. Above 100° C. for acetone, $1 >> bP_i$, which results in the elimination of the second adsorption constant, or b may be set equal to zero in the above equations. That the adsorption correction is significant at lower temperatures with acetone is largely due to the nature of the Burnett apparatus, which roughly multiplies errors of this type by the number of expansions, l, in a given run. Compressibilities at the higher pressures are particularly vulnerable, since Z_i depends on $l - i + 1$ pressure readings.

In addition to the adsorption correction, the data were also corrected for certain pressure heads, expansion of the metal cell walls due to pressure, gravitational effects influenced by the local gravitational constant, changes in ambient temperature, and the buoyancy of air.

EXPERIMENTAL RESULTS

Compressibilities. Acetone compressibility factor results for the temperature range of 25° to 150° C. at 25° C. intervals were divided into three progressive stages. The first stage is the collection of raw Burnett data—the experimental pressure sequence for each run at each temperature. These data (deposited with ADI) yield $P_i N^i$ curves typified by Figure 3 because of the presence of adsorption. Next, each data run was corrected for adsorption by the method outlined above resulting in the second stage (corrected but unsmoothed data also deposited with ADI). Figure 4 shows these results for the three runs at 100° C. Except for some scatter near zero pressure, the adsorption correction provides a smooth Z-P curve for the data of Run III of Figure 3. The smoothed data (stage three) appearing in Table II were obtained from first smoothing the corrected data for each isotherm with four experimental runs at 25° C., four at 50° C., two at 75° C., three at 100° C., three at 125° C., and two at 150° C. Next, these "best" Z-P curves for each isotherm were crossplotted on Z *vs.* T, $(\partial Z/\partial P)_T$ *vs.* P, $(\partial Z/\partial T)_P$ *vs.* P, $(\partial Z/\partial P)_T$ *vs.* T, and $(\partial Z/\partial T)_P$ *vs.* T graphs where the final data smoothing was performed. The final smoothed Z-P curve of the 100° C. isotherm (Figure 4) is above the majority of the corrected data points, because of this final smoothing procedure.

Comparison of the maximum pressure for each isotherm of Table II with the saturation pressure of Stull (*24*) and the International Critical Tables (*11*) reveals that only 60 to 80% of the saturation pressure was obtained. In the case of the 100°, 125°, and 150° C. isotherms, data to about 95% of the saturation pressure were taken but are not reported here.

To estimate the maximum uncertainty in the results of Table II, systematic errors were considered due to the value of the apparatus constant, the determination of P_0/Z_0 including the adsorption correction, the measurement of pressure and temperature, and the smoothing procedure.

The maximum uncertainty in the apparatus constant was 0.007%; the uncertainty was estimated as l times 0.007%, where l was the average number of expansions at a given temperature. Estimates of the error in P_0/Z_0 were calculated to be as follows: 0.15% at 25° C., 0.12% at 50° C., 0.03% at 75° C., 0.011% at 100° C., 0.010% at 125° C., and 0.010% at 150° C. Uncertainty due to pressure and temperature was estimated from the equation

$$dZ = \left(\frac{\partial Z}{\partial P}\right)_T dP + \left(\frac{\partial Z}{\partial T}\right)_P dT \qquad (14)$$

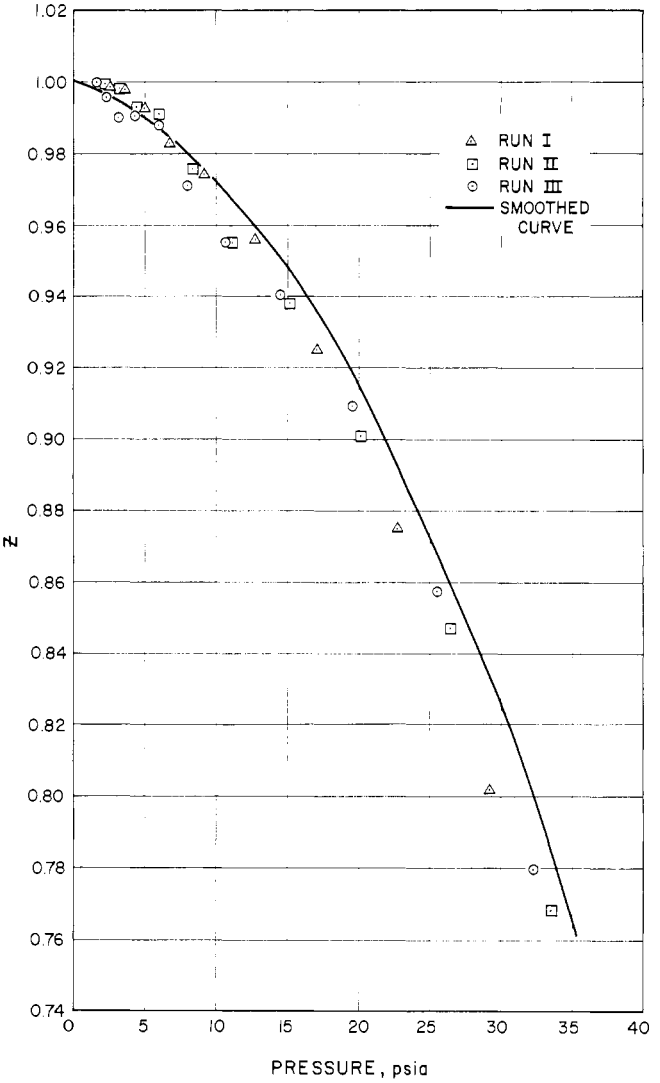

Figure 4. Compressibility factor–pressure diagram for acetone data after adsorption correction, 100° C., all runs

with values of the partial derivatives obtained from the smoothing graphs. The maximum value of 0.026% was used for all temperatures. Addition of uncertainties results in the values of Table III.

The transition from adsorption-corrected data for individual runs to the smoothed compressibility factors of Table II results in a standard error of estimate of the experimental points by the smooth curve of 0.92% for 25° C., 1.51 for 50° C., 0.58 for 75° C., 1.07 for 100° C., 1.37% for 125° C., and 0.59% for 150° C. For individual isotherms the standard error of estimate of the best curve is of the order of the uncertainties listed in Table III. The higher values for the smooth curves (Table II) are due to the final smoothing procedure which results in limited shifting of the entire isotherm as illustrated by Figure 4 for the 100° C. data. The inability of the present adsorption correction method to treat data over a wide temperature range necessitates the final smoothing procedure.

Virial Coefficients. The present apparatus is particularly suitable for securing virial coefficients of polar gases because of low pressure capability (to 1 p.s.i.a.) necessary for zero pressure extrapolations and moderate pressure capability necessary for prediction of virials higher than the second. Second, third, and fourth Berlin virial coefficients were obtained by the usual graphical method from the compressibilities of Table II:

Table II. Acetone Compressibility Factors

Pressure, P.S.I.A.	Z_{exptl}	Pressure, P.S.I.A.	Z_{exptl}
25° C.		125° C.	
3.0	0.9742	60.0	0.8001
2.0	0.9855	56.0	0.8216
1.0	0.9935	52.0	0.8428
		48.0	0.8630
50° C.		44.0	0.8833
		40.0	0.9016
		36.0	0.9175
6.0	0.9535	32.0	0.9315
5.0	0.9654	28.0	0.9443
4.0	0.9750	24.0	0.9558
3.0	0.9830	20.0	0.9660
2.0	0.9896	18.0	0.9710
1.0	0.9950	16.0	0.9756
		14.0	0.9797
75° C.		12.0	0.9833
		10.0	0.9868
		8.0	0.9900
16.0	0.8533	6.0	0.9928
15.0	0.8727	4.0	0.9954
12.0	0.9187	2.0	0.9978
9.0	0.9515		
6.0	0.9751		
5.0	0.9810		
4.0	0.9859		
3.0	0.9900		
2.0	0.9937	150° C.	
		105.0	0.7882
		99.0	0.8091
100° C.		93.0	0.8288
		87.0	0.8478
		81.0	0.8658
35.0	0.7650	75.0	0.8827
30.0	0.8251	69.0	0.8983
28.0	0.8450	63.0	0.9126
25.0	0.8731	57.0	0.9256
23.0	0.8909	51.0	0.9385
20.0	0.9151	45.0	0.9505
18.0	0.9288	39.0	0.9609
15.0	0.9477	33.0	0.9696
13.0	0.9600	27.0	0.9770
10.0	0.9725	21.0	0.9833
8.0	0.9805	18.0	0.9862
6.0	0.9871	15.0	0.9887
4.0	0.9924	12.0	0.9912
3.0	0.9945	9.0	0.9934
2.0	0.9964	6.0	0.9958
		3.0	0.9979

Table III. Per Cent Estimated Maximum Uncertainty of Adsorption-Corrected Data

25° C.	50° C.	75° C.	100° C.	125° C.	150° C.
0.20	0.20	0.10	0.09	0.10	0.10

Table IV. Berlin Virial Coefficients for Acetone

Temp., °C.	$-B^1 \times 10^2$, (P.S.I.A.)$^{-1}$	$-C^1 \times 10^3$, (P.S.I.A.)$^{-2}$	$-D^1 \times 10^5$, (P.S.I.A.)$^{-3}$
25	0.5930	0.530	14.5
50	0.4265	0.270	4.9
75	0.2875	0.120	1.70
100	0.1755	0.048	0.30
125	0.1070	0.023	0.0075
150	0.0700	0.012	0.0000

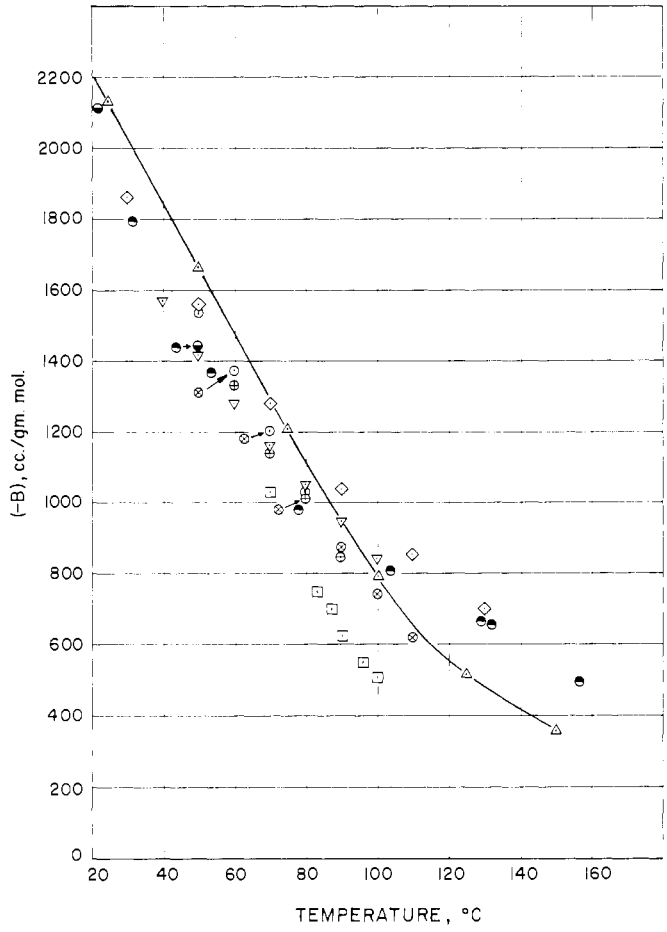

Figure 5. Second virial coefficients

$$B^1 = \lim_{P \to 0} \frac{Z - 1}{P} \tag{15}$$

$$C^1 = \lim_{P \to 0} \frac{|(Z-1)/P| - B^1}{P} \tag{16}$$

and D^1 is the zero pressure slope of $\{[(Z - 1)/P] - B^1\}/P$. The results are presented in Table IV. Use of these virial coefficients in Equation 1 provides a fit of experimental compressibilities within the uncertainties of Table III. Because of contributions from virials higher than the fourth, extrapolation to pressures higher than those of Table II is not recommended.

For comparison with other investigations, Leiden second virial coefficients B were computed from

$$B = B^1 RT \tag{17}$$

where

$$Z = 1 + \frac{B}{V} + \frac{C}{V^2} + \frac{D}{V^3} + \ldots \tag{18}$$

The results are compared with those of Lambert, Roberts, Rowlinson, and Wilkinson (*13*), Eucken and Meyer (*9*), Bottomley and Spurling (*5, 6*), Abbott (*1*), Zaalishvili and Koyysko (*29, 30*), and Zaalishvili and Belousova (*28*) in Figure 5.

Stockmayer Force Constants. An attempt was made to calculate Stockmayer force constants (*23*) from the present second virial values and the complete equation for B as a function of the constants as given by Buckingham and Pople (*7*). A reasonably good fit of B of 11% average deviation was obtained only at $\sigma = 3.74$ A, $(\epsilon/k) = 80°$ K., and $t^* = [\mu^2/(8)^{1.2}(\epsilon\sigma^3)] = 5.06$. These values are both physically unreasonable and fail to compare with those of Rowlinson (*20*) from the above cited second virial results of Lambert *et al.* or those of Monchick and Mason (*16*) from gas viscosity data.

As noted by Pople (*19*), second virial coefficient data for strongly associated polar gases such as the alcohols and ketones are generally not well fitted by the Stockmayer model over a significant temperature range and/or the optimum value of the force constants lose physical significance. A good fit of the data does not guarantee the model to be correct. Theoretical calculations with the equations presented by Buckingham and Pople indicate that induced dipole, quadrupole, and steric interactions are important for acetone at the present temperatures. The Stockmayer model with only the dipole-dipole interaction superimposed on the Lennard-Jones model is thus inadequate for the present temperatures.

Association. The highest isotherm, 150° C., is considerably below the maximum temperature, 250° C., of which the apparatus is capable. Experimental work was halted at 175° C. with the appearance of a yellowish liquid as condensate from the cell. Analysis of this liquid by the Celanese Chemical Co. indicated that a high degree of association had occurred: 3.0% diacetone alcohol, 0.13% mesityl oxide, 0.01% phorone, and 0.62% various unidentified compounds together with the original impurities listed previously.

The presence of dimers and trimers was not unexpected, as Eucken and Meyer and Lambert *et al.* had proposed a model to determine the fraction of the dimers α quantitatively from

$$\frac{\alpha}{2} = \frac{P}{K_P} \tag{19}$$

and

$$B = b_0 - RT/K_P = b_0 - RT \exp[(-\Delta S_2/R) + (\Delta H_2/RT)] \tag{20}$$

as given by Weltner and Pitzer (*26*), where b_0 is the covolume of Eucken and Meyer, ΔH_2 the heat of dimerization, and ΔS_2 the change in entropy. Values of dimerization equilibrium constant, K_P, in atmospheres and the heat of dimerization, ΔH_2, are listed in Table V as computed from the present second virial coefficients.

Figure 6 compares K_P with values obtained from the heat capacity data of Kobe and Pennington (*12*) and also from the analysis at 175° C. cited above. Consistent with Equation 20, Weltner and Pitzer provided the following equations from which K_P may be computed from C_P data:

$$C_P = C_P^\circ + aP \tag{21}$$

and

Table V. Results of Dimerization Calculations

Temp., °K.	$\log_{10} K_P$
298.15	1.04
323.15	1.18
348.15	1.34
373.15	1.54
398.15	1.73
423.15	1.88

$\Delta\bar{H}_2 = -3.9$ kcal./gm.mol.
$\Delta\bar{S}_2 = -17.7$ cal./gm.mol.-°K

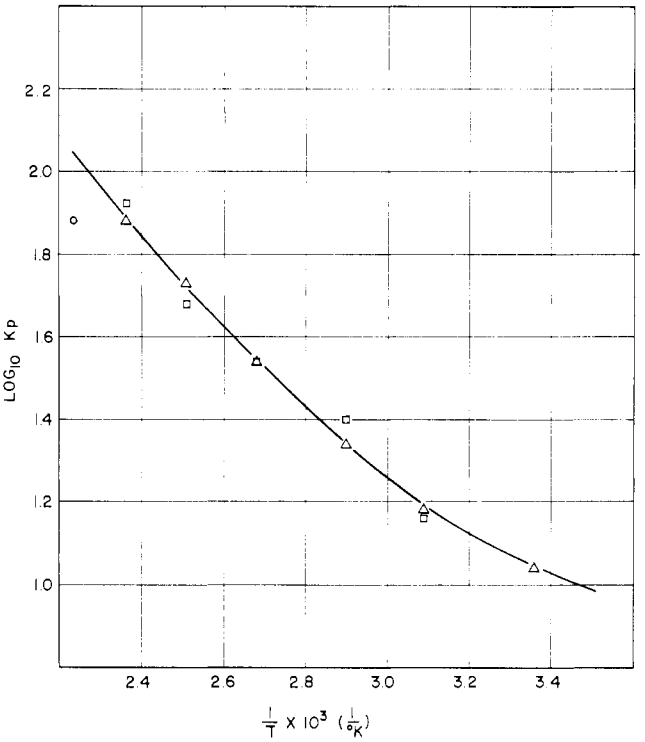

Figure 6. Association equilibrium constants
△ Computed from B data
□ C_P data (*10*)
○ GC analysis

$$a = \frac{\Delta H_2^2}{RT^2} \exp[(-\Delta S_2/R) + (\Delta H_2/RT)] = \frac{\Delta H_2^2}{RT^2 K_P} \tag{22}$$

Polar Correlation. The polar correlation of Eubank and Smith (Equation 5) was checked against the acetone compressibilities at various values of the constant c. The average absolute deviation for all six isotherms over the entire pressure range of the data was 2.6% with $c = 0.7$ and 2.2% with $c = 0.8$—the best fit. This result is in reasonable agreement with the best value of $c = 0.7$ of Eubank and Smith from a fit of their experimental enthalpy data.

ACKNOWLEDGMENT

The authors acknowledge the continued support of the National Science Foundation through grants GP-2188 and GK-711.

NOMENCLATURE

B = Leiden second virial coefficient, cc./g. mole
B^1 = Berlin second virial coefficient, (p.s.i.a.)$^{-1}$
C = Leiden third virial coefficient, (cc./g. mole)^2
C^1 = Berlin third virial coefficient, (p.s.i.a.)$^{-2}$
C_P = heat capacity, cal./g. mole-° K.
D = Leiden fourth virial coefficient, (cc.. mole)^3
D^1 = Berlin fourth virial coefficient, (p.s.i.a.)$^{-3}$
ΔH_2 = heat of dimerization, cal./g. mole
K_P = equilibrium constant for dimerization, atm.
N = apparatus constant, $(V_1 + V_2)/V_1$
P = pressure, p.s.i.a.
P^* = polar parameter
R = gas constant
S = surface area
ΔS_2 = entropy change on dimerization, cal./g. mole-° K.
S_a = ratio of surface areas, $(S_1 + S_2)/S_1$
T = temperature, ° K. or ° C.
U_0 = limiting value of pressure ratio at zero pressure
V = volume, cc./g. mole

W = first adsorption constant, temperature-dependent
Z = compressibility factor
a = constant in heat capacity equation, cal./g. mole-° K.-atm.
b = coefficient in Langmuir adsorption model, p.s.i.a.$^{-1}$
b_0 = volume of Eucken and Meyer, cc./g. mole
k = Boltzmann constant
l = total number of expansions
t^* = parameter in Stockmayer model, $\mu^{*2}/(8)^{1/2}$

Greek Letters

α = fraction of dimers
ϵ/k
and
σ = Stockmayer force constants
μ^* = reduced dipole moment, $\mu/(\epsilon\sigma^3)^{1/2}$
μ = dipole moment
ω = acentric factor of Pitzer

Subscripts

a = ambient conditions
i = integer indicating number of expansion
j = integer indicating number of expansion
r = variable divided by critical value

LITERATURE CITED

(1) Abbott, M.M., Ph.D. dissertation, Rensselaer Polytechnic Institute, Troy, N. Y., 1965.
(2) Anderson, L.N., M.S. thesis, Texas A&M University, College Station, Tex., 1965.
(3) Anderson, L.N., Ph.D. dissertation, Texas A&M University, College Station, Tex., 1967.
(4) Barb, D.K., M.E. report, Texas A&M University, College Station, Tex., 1964.
(5) Bottomley, G.A., Spurling, T.H., *Australian J. Chem.* **20**, 1789 (1967).
(6) Bottomley, G.A., Spurling, T.H., *Nature* **195**, 900 (1962).
(7) Buckingham, A.D., Pople, J.A., *Trans. Faraday Soc.* **51**, 1173 (1955).
(8) Eubank, P.T., Smith, J.M., *A.I.Ch.E. J.* **8**, 117 (1962).
(9) Eucken, A., Meyer, L., *Z. physik. Chem.* **B5**, 452 (1929).
(10) Holborn, L., Otto, J., "Handbuch der Experimentalphysik," Vol. **V112**, p. 144, Akademische Verlagsgesellschaft, Leipzig, 1929.
(11) International Critical Tables of Numerical Data, Physics, Chemistry and Technology, Vol. **III**, pp. 218, 239, McGraw-Hill, New York, 1933.
(12) Kobe, K.A., Pennington, R.E., *J. Am. Chem. Soc.* **79**, 300 (1957).
(13) Lambert, J.D., Roberts, G.A.H., Rowlinson, J.S., Wilkinson, V.J., *Proc. Roy. Soc. (London)* **A196**, 113 (1945).
(14) Langmuir, I., *J. Am. Chem. Soc.* **38**, 2221 (1916).
(15) Michels, A., Wouters, H., *Physica* **8**, 923 (1941).
(16) Monchick, L., Mason, E.A., *J. Chem. Phys.* **35**, 1692 (1961).
(17) Moreland, M.P., Ph.D. dissertation, University of Texas, Austin, Tex., 1966.
(18) Mueller, W.H., Leland, T.W., Jr., Kobayashi, R., *A.I.Ch.E. J.* **7**, 267 (1961).
(19) Pople, J.A., *Proc. Roy. Soc. (London)* **A221**, 498 (1954)
(20) Rowlinson, J.S., *Trans. Faraday Soc.* **45**, 974 (1949).
(21) Schneider, W.G., Duffie, J.A.H., *J. Chem. Phys.* **17**, 751 (1949).
(22) Silberberg, I.H., McKetta, J.J., Kobe, K.A., J. CHEM. ENG. DATA **4**, 314 (1959).
(23) Stockmayer, W.H., *J. Chem. Phys.* **9**, 398 (1941).
(24) Stull, D.R., *Ind. Eng. Chem.* **39**, 517 (1947).
(25) Suh, K.W., Storvick, T.S., *A.I.Ch.E. J.* **13**, 231 (1967).
(26) Weltner, W., Pitzer, K.S., *J. Am. Chem. Soc.* **73**, 2606 (1951).
(27) Wiebe, R., Gaddy, V.L., Heins, C., *Ibid.*, **53**, 1721 (1931).
(28) Zaalishvili, Sh.D., Belousova, Z.S., *Zhur. Fiz. Khim.* **38**, 503 (1964).
(29) Zaalishvili, Sh.D., Kolysko, L.E., *Ibid.*, **34**, 2596 (1960).
(30) *Ibid.*, **35**, 2613 (1961).

RECEIVED for review September 25, 1967. Accepted March 15, 1968. Material supplementary to this article has been deposited as Document 10026 with the ADI Auxiliary Publications Project, Photoduplication Service, Library of Congress, Washington, D. C. 20540. A copy may be secured by citing the document number and by remitting $2.50 for photoprints or $1.75 for 35-mm. microfilm. Advance payment is required. Make checks or money orders payable to Chief, Photoduplication Service, Library of Congress.

Osmotic Properties of Some Aqueous Electrolytes at 60° C.

WILLIAM T. HUMPHRIES, CARL F. KOHRT, and C. STUART PATTERSON
Department of Chemistry, Furman University, Greenville, S. C. 29613

A modified isopiestic apparatus is described that performs satisfactorily at temperatures below 100° C. Isopiestic ratios to NaCl are reported for KBr, KCl, and Na_2SO_4 in H_2O at 60° C. over a wide concentration range. The ratios for KCl and KBr agree well with published data. Plots of R vs. T for KCl and Na_2SO_4 show agreement with lower temperature data, but reveal significant inconsistencies with data at higher temperatures.

AN attempt was made to extend the isopiestic method into the range between ambient and 100° C. (2). That attempt was modestly successful at 45° C. (2), but the apparatus and procedures were clearly not adequate for higher temperatures.

The purpose of this paper is to describe a modified apparatus and procedure, which appear to be highly satisfactory at least up to 80° C., and to report the osmotic properties of aqueous KCl, KBr, and Na_2SO_4 solutions over a wide concentration range at 60° C.

EXPERIMENTAL

A ⅜-inch Plexiglass plate, *1*, holding Teflon lids, *2*, (nylon lids varied widely in "dry weight" after equilibration) is connected by a threaded Teflon collar, *3*, to a nylon drive screw, *4*, that runs to the bottom of a 250-mm. Kimax vacuum desiccator, *5* (Figure 1). A similar Plexiglass plate, *6*, rests on a 2-inch thick gold-plated copper block, *7*, and serves to hold 1-inch diameter gold-plated silver cups, *8*, in place. The cups rest directly upon the copper block. A lever arm, *9*, with a Teflon-coated horseshoe magnet, *10*, at each end is located at the top of the drive screw. To lower the lids, one rotates the lever arm counterclockwise using a magnet so that the lid holder will move down the drive screw. Three Teflon-coated steel rods, *11*, mounted in the copper block guide the lid holder downward and prevent it from turning with the screw. The holes in the lid holder are larger than the diameter of a cup. As each lid comes into contact with its cup, the lid holder con-